

Dynamical Collective Memory in Fluidized Granular Materials

A. Plati,¹ A. Baldassarri,² A. Gnoli,² G. Gradenigo,³ and A. Puglisi²

¹*Dipartimento di Fisica, Università di Roma Sapienza, P.le Aldo Moro 2, 00185, Rome, Italy*

²*Istituto dei Sistemi Complessi—CNR and Dipartimento di Fisica, Università di Roma Sapienza, P.le Aldo Moro 2, 00185, Rome, Italy*

³*NANOTEC—CNR and Dipartimento di Fisica, Università di Roma Sapienza, P.le Aldo Moro 2, 00185, Rome, Italy*

 (Received 21 January 2019; revised manuscript received 30 April 2019; published 17 July 2019)

Recent experiments with rotational diffusion of a probe in a vibrated granular media revealed a rich scenario, ranging from a dilute gas to a dense liquid with cage effects and an unexpected superdiffusive behavior at large times. Here we set up a simulation that reproduces quantitatively the experimental observations and allows us to investigate the properties of the host granular medium, a task not feasible in the experiment. We discover a persistent collective rotational mode which emerges at a high density and a low granular temperature: a macroscopic fraction of the medium slowly rotates, randomly switching direction after very long times. Such a rotational mode of the host medium is the origin of the probe's superdiffusion. Collective motion is accompanied by a kind of dynamical heterogeneity at intermediate times (in the cage stage) followed by a strong reduction of fluctuations at late times, when superdiffusion sets in.

DOI: [10.1103/PhysRevLett.123.038002](https://doi.org/10.1103/PhysRevLett.123.038002)

Introduction.—Granular media are systems made of macroscopic particles, shortened “grains,” whose diameter usually exceeds the hundreds of microns, ideally without an upper limit [1,2]. A typical list of granular materials includes sand, powders, cereals, cements, and pharmaceuticals, but in certain contexts it may incorporate planetary rocks such those in Saturn's rings [3]. The study of granular media originates from the several applications in chemistry, material sciences and in the management of geophysical hazards. For several decades, however, it has become a fertile inspiration for theoretical physics, particularly in the framework of nonequilibrium statistical mechanics [4–6]. In fact, grains can be described as particles which interact dissipatively [7]. Even in dilute conditions and under strong vibrofluidization, the resemblance between a granular gas and a molecular gas is deceptive, hiding important dynamical differences [8]. When packing fraction increases or external energy input decreases, the dissipative nature of granular interactions becomes more and more relevant, making the paradigms of equilibrium statistical physics inapplicable [9].

A state of driven granular matter which has received less attention than others is the liquid one, i.e., a regime of steady agitation, loosely interpreted as “ergodic,” where the spatial arrangement of grains is not a crystal but still shows some degree of order as in molecular liquids [10,11]. Granular liquids, because of dissipative interactions, display spatial correlations in the velocity field, a property which leads to strong violations of the fluctuation-dissipation relation and to interesting memory effects [12–14]. Another common granular feature is the lack of energy equipartition, for instance in the inhomogeneity of “granular temperature” measured along different directions in an anisotropic setup [15].

Recently, some of us have conducted a series of experiments with vibrofluidized granular materials, using a blade rotating around a suspended vertical axis as a sort of granular Brownian probe [see Fig. 1(a)] [16]. When the occupied volume fraction is low and vibration is strong, the medium behaves as a gas and the probe displays the typical ballistic-diffusive behavior in the angular mean squared displacement [msd, see Fig. 1(d)]. At high density and weak vibration, the medium becomes a cold liquid and the msd reveals cage effects typical of attempted dynamical arrest. Most importantly, superdiffusion is observed at time delays larger than the onset of the transient cage effect. Filtering out high frequencies of the probe's angular velocity, one sees a surprisingly long dynamical memory, which may induce quasiballistic (angular) flights of the probe for times of the order of tens of seconds [see Figs. 1(b) and 1(c)]. Up to now only phenomenological models have caught this behavior [17], leaving unexplored its microscopic origin, which certainly resides in the unconventional dynamics of the granular host medium. Indeed, a crucial element of those simplified models is an emergent, effective, giant momentum of inertia of the probe, which may compare with that of the whole granular system. Analogies may be found in recent experimental works, where persistent collective motion [18,19] or anomalous diffusion [11] have been observed in vibrofluidized granular materials made of anisotropic particles, a crucial difference with the work discussed here. In this Letter we reproduce the experimental observations for the probe through a 3D discrete-elements model of the real setup including the grains' rotations and dissipation through normal and tangential interactions. After having shown the quantitative agreement between simulations and the experiment, we focus on the granular medium

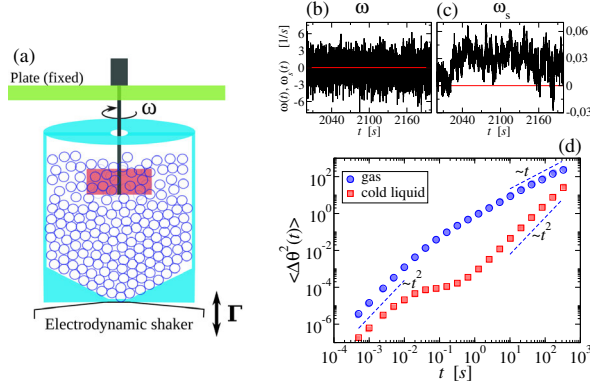


FIG. 1. (a) Setup of the experiment and of the simulation. (b) and (c) A sample of the $\omega(t)$ signal (left) and its filtered “slow-component” $\omega_s = (1/\tau) \int_t^{t+\tau} \omega(t') dt'$ (with $\tau = 2$ seconds) when $N = 2600$ and $\Gamma = 26.8$. (d) msd in a gaslike case ($N = 350$ and $\Gamma = 39.8$) and in the cold-liquid case ($N = 2600$ and $\Gamma = 26.8$) with both cage effects and late-time superdiffusion.

alone. Our results give direct evidence of a collective dynamical memory, originated in a kind of synchronization between grains movements over long timescales.

Experimental and numerical setup.—The experiment, realized in Ref. [16], is sketched in Fig. 1(a). Here we report the results of a numerical simulation which is meant to reproduce the setup (container, grains, and rotator) in its spatial and temporal proportions. Both the real and the simulated systems consist of a cylinder-shaped recipient (diameter 90 mm, maximum height 47 mm, and total volume 245 cm³), with an inverse-conical-shaped base, containing a number N of steel spheres (diameter 4 mm, mass 0.27 g), representing the “granular medium.” The recipient is vertically vibrated: the real system was mounted on an electrodynamic shaker fed with a noisy signal (spectrum approximately flat in the range 200–400 Hz and roughly empty outside that range), in the simulated system instead the container is vibrated with a sinusoidal law for its top vertical position $A \sin(2\pi\nu t)$, with a constant frequency $\nu=200$ Hz and amplitude $A \in [0.03, 0.25]$ mm. We recall that the maximum vertical acceleration (divided by gravity g) Γ varies in the range 20–40 and the maximum vertical velocity in 80–300 mm/s. The effect of the shaking is the fluidization of the granular medium, which—depending on N and Γ —stays in a steady gas or liquid regime. The probe for diffusion is a blade (dimensions 35×6×15 mm, momentum of inertia $I=353$ gmm²) mechanically isolated from the container, which can rotate around a centered vertical axis and takes energy only from collisions with the granular medium. The angular velocity $\omega(t)$ of the blade and its absolute angle of rotation $\theta(t) = \int_0^t \omega(t') dt'$ are measured in the experiment by an encoder with high spatial and temporal resolution (see Supplemental Material in Ref. [16]). The numerical simulations are performed with a discrete-elements model implemented by LAMMPS package [20] with interactions

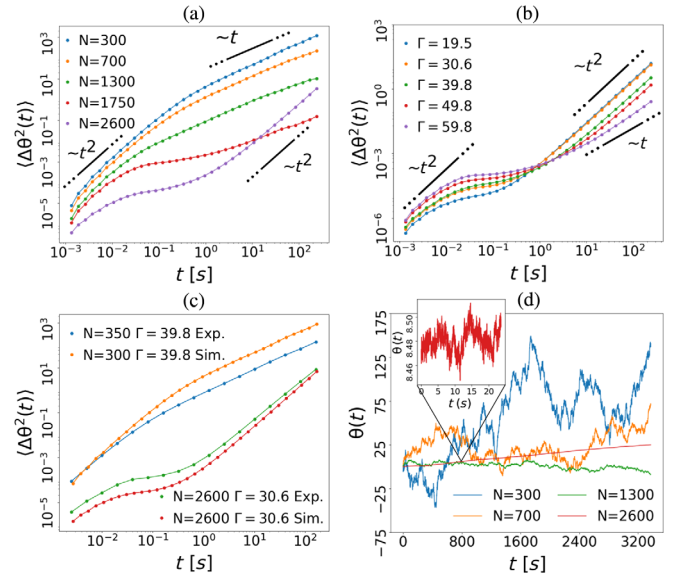


FIG. 2. Dynamics of the probe. (a) msd in simulations with $\Gamma = 39.8$ and different values of N . (b) msd in simulations with $N = 2600$ and different values of Γ . (c) msd, comparison with experiments. (d) Trajectories $\theta(t)$ in several simulations with $\Gamma = 39.8$ and different values of N .

obeying a nonlinear viscoelastic Hertzian model that takes into account the relative deformation of the grains. In order to properly reproduce the soft collision dynamics, simulations run with a time step of $\sim 10^{-5}$ s. Our macroscopic phenomena occur on timescales larger than 10 s; therefore we integrate the dynamics for total times $t_{\text{TOT}} = 3.6 \times 10^3$ s, spanning more than eight decades of time steps. More details about the simulation, including the parameters that control the dissipative and the elastic contributions of the interaction, are given in the Supplemental Material [21]. There the reader can also find a table with the correspondence between N and best estimates of the packing fraction ϕ . We stress that, in view of the collective nature of the phenomena studied here, it is reasonable to expect a certain robustness of the results with respect to the microscopic details. Indeed, the main experimental phenomena are qualitatively reproduced in large regions of the parameters’ space. The effects of changing the dissipation of interactions, the mass, or the diameter of particles are discussed in the Supplemental Material [21]. Here we focus on the particular set of values exhibiting the optimal quantitative agreement (within a tolerance of roughly 10%) with the experiment.

Numerical results: study of the probe.—We first compare numerical and experimental results for velocity fluctuations $\langle \omega^2 \rangle - \langle \omega \rangle^2$ (proportional to probe’s kinetic temperature), not shown here, which fairly agree in the whole range of values of N and Γ . In Figs. 2(a) and 2(b), we show the results of the crucial test of our simulation, i.e., the msd in many different situations. When N is small and Γ is high [cyan, yellow, and green curves in Fig. 2(a)] the granular

medium provides the blade with uncorrelated impacts and the large mass of the probe is sufficient to predict a leading order Ornstein-Uhlenbeck behavior [36,37]; this determines the typical ballistic ($\text{msd} \sim t^2$) to diffusive ($\text{msd} \sim t$) scenario. When N increases the medium entraps the probe—similarly to the cage effect in molecular liquids—resulting in a transient arrest of the msd at intermediate times $t \sim t_{\text{cage}}$, followed by the usual “escape” with the behavior $\text{msd} \sim t$ when $t \gg t_{\text{cage}}$ [red curve in Fig. 2(a), purple curve in Fig. 2(b)]. A peculiar granular feature is the possibility to develop late-time superdiffusive behavior, when N is increased further [purple curve in Fig. 2(a)] or Γ reduced further [cyan, yellow, green, and red curves in Fig. 2(b)]. At the smallest values of Γ we observe the limit case $\text{msd} \sim t^2$ when $t \gg t_{\text{cage}}$. In Fig. 2(c) we demonstrate the good comparison, appreciable also at the quantitative level, between the msd observed in the simulations and in the experiments, in two very different cases. Finally, in Fig. 2(d) we show some examples of the numerical time series $\theta(t)$ (along ~ 1 hour) when N is tuned from the dilute gas to the dense liquid (constant Γ). This plot reveals the significant change in the probe’s dynamics induced by the variation of surrounding granular density. We remind that dissipative interactions naturally reduce velocity fluctuations when N is raised at constant Γ . Besides this, a nontrivial memory effect clearly emerges, with long relaxation times evident in the persistence of the direction of motion.

Numerical results: study of the medium.—Once the simulation has been successfully compared with the experimental results, we can obtain new information which was unreachable experimentally, due to the 3D nature of the setup. Our first focus is on the most natural collective variables which could be coupled to the angular velocity of the blade, that is, the average angular velocity of the granular medium (with respect to the central axis)

$$\Omega_c(t) = \frac{1}{N} \sum_{i=1}^N \dot{\theta}_i(t) \quad (1a)$$

$$\theta_i(t) = \arctan\left(\frac{y_i(t)}{x_i(t)}\right) \quad \dot{\theta}_i(t) = \frac{\left(\mathbf{r}_i(t) \times \mathbf{v}_i(t)\right)_z}{r_i^2}, \quad (1b)$$

and its time-integral which represents a collective absolute angle $\Theta_c(t) = \int_0^t \Omega_c(t') dt'$.

A solid evidence that $\Theta_c(t)$ is meaningful with respect to the anomalous diffusive properties of the probe can be found in Fig. 3. Figure 3(a) reports the parametric plot $\theta(t)$ (blade’s angle) vs $\Theta_c(t)$ (collective angle). It is immediately clear that a sort of crossover line exists in the plane of parameters N, Γ (with, in fact, a weak dependence on Γ coordinate); for small values of N and high values of Γ one has a phase where $\theta(t)$ and $\Theta_c(t)$ are mostly uncorrelated.

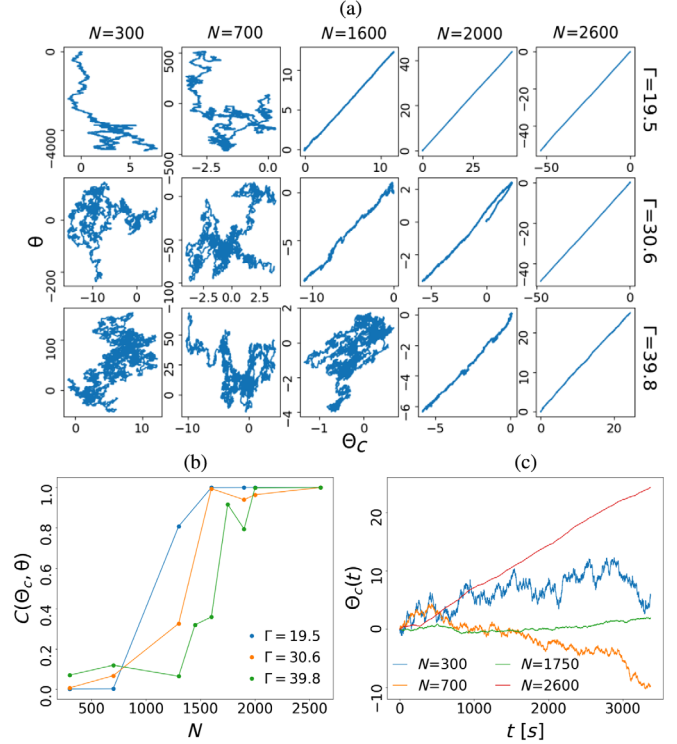


FIG. 3. Comparison probe vs collective rotation of the granular medium. (a) Parametric plot of the two rotations for several choices of N and Γ . (b) Correlation between the probe and the collective rotation as a function of N for different Γ . (c) Simulation without the probe, absolute collective angle Θ_c vs t for different N at $\Gamma = 39.8$.

On the contrary, for large N and small Γ a strong correlation emerges between the two signals. In Fig. 3(b) we show a covariance $C(\Theta_c, \theta)$ defined as

$$C(x, y) = 1 - \frac{\langle [x'(t) - y'(t)]^2 \rangle}{\langle (x'(t))^2 \rangle + \langle (y'(t))^2 \rangle}, \quad (2)$$

with $x'(t) = x(t) - \langle x \rangle$, $y'(t) = y(t) - \langle y \rangle$ and the average runs over data sampled for the whole simulation time (typical simulation times are 3600 s with a temporal step $\Delta t = 1.35 \times 10^{-5}$ s). Note that this estimator of the covariance can also be rewritten as $C(x, y) = 2\langle x'(t)y'(t) \rangle / \{ \langle [(x'(t))^2] \rangle + \langle [(y'(t))^2] \rangle \}$. Figure 3(b) confirms that it can be interpreted as an order parameter distinguishing between those two phases, and that the crossover occurs, with a fair sharpness, at a value $N_c \sim 1300$ –1600 only weakly dependent upon Γ .

The results of the previous analysis make clear that in the dense and cold cases, when seen from the point of view of large timescales ($\gtrsim 1$ s, roughly speaking), the dynamics of the blade is strongly correlated to the collective rotation of the granular medium, which is the real hallmark of the transition. This suggests to us to focus on a new series of simulations *without* the rotating blade, with the aim of

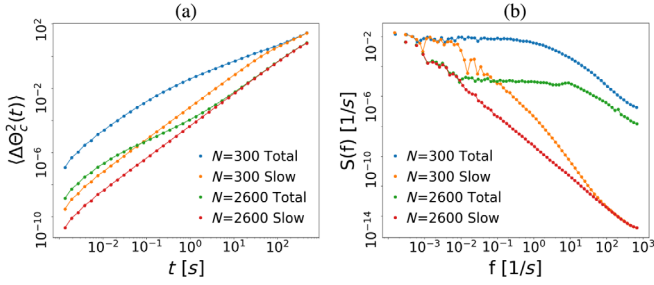


FIG. 4. Collective variable $\Theta_c(t)$ at two different values of N and $\Gamma = 39.8$, compared with its “slow component,” see text for definition. (a) msd; (b) power spectra of Ω_c .

focusing upon the granular medium itself [38]. The analysis of $\Theta_c(t)$ in these “blade-free” simulations, shown in a few relevant cases in Fig. 3(c), immediately corroborates this intuition: the collective absolute angle of the granular medium is erratic and Brownian-like for $N < N_c$ and much more smooth at $N > N_c$. In particular the cases at $N > N_c$ appear constituted by long periods where Θ_c travels in a constant direction, interrupted by rare turns. The average time t_{coll} between those turns seem to increase with N , up to a point (case at the largest available $N = 2600$, red curve) where it is longer than the whole simulation. We also ran longer simulations, not shown here, confirming that sudden turns occur also at $N = 2600$, but with $t_{\text{coll}} \gg 10^3$ seconds. The interesting connection between spatial rearrangements and changes of rotation speed or direction has eluded our attempts and remains an open question for future investigations.

As expected from the strong correlation between $\theta(t)$ and $\Theta_c(t)$, for $N > N_c$, the large-time behavior of the msd of $\Theta_c(t)$ is superdiffusive exactly as already seen for the probe, see Fig. 4(a). We have also verified, see the Supplemental Material [21], that the distributions of angular displacements at times larger than t_{cage} are always close to Gaussian, ruling out large tails such as those in Ref. [22]. Superdiffusive behavior is therefore caused by the long persistent angular drifts discussed before. The connection is the following: in the dense cases t_{coll} becomes huge; therefore what we call “large times,” with respect to microscopic and intermediate (t_{cage}) timescales, are actually “small times” with respect to t_{coll} . Only following the signal for times much longer than t_{coll} one would recover the asymptotic (or “final”) diffusive behavior $\text{msd} \sim t$. In order to focus on the dynamics at timescales $\sim t_{\text{coll}}$, we get rid of the smaller timescale t_{cage} by defining the slow collective velocity $\Omega_s(t) = (1/\tau) \int_t^{t+\tau} \Omega_c(t') dt'$, with τ larger than t_{cage} (for instance $\tau = 1.35$ s). Defining, analogously, the slow component of $\Theta_c(t)$, i.e., $\Theta_s(t) = \int_0^t \Omega_s(t') dt'$ gives also the possibility of looking at the collective msd when the fast position oscillations are filtered out, see again Fig. 4(a). The slow component, surprisingly, has always a persistent ballisticlike motion, even in the most dilute cases.

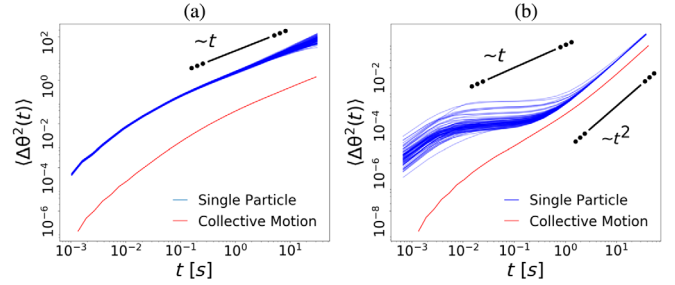


FIG. 5. Mean squared displacement of ~ 100 particles spread randomly in the system, in a dilute case and a dense case, with same parameters as those in Fig. 4.

However, in the diluted cases, this ballistic motion is a very weak signal and does not appear in the msd of the total variable. The same observation can be seen for the power spectrum of the angular velocity Ω_c which is defined as $S(f) = (1/2\pi t_{\text{TOT}}) |\int_0^{t_{\text{TOT}}} \Omega_c(t) e^{i(2\pi f)t} dt|^2$ [16], shown in Fig. 4(b). In both dilute and dense cases the slow component (yellow and red curves) has a Lorentzian-shaped spectrum, with a flat part at small frequencies f and a decaying part, roughly $\sim f^{-2}$ at larger frequencies. Only in the dense case $N = 2600$ such a low-frequency “flat” part intervenes at very small frequencies, so that part of $\sim f^{-2}$ emerges in the total signal. We verified that changing τ around a value slightly larger than t_{cage} does not affect this scenario.

The last question we address concerns fluctuations, which may be crucial to define a proper correlation length. In glassy systems a well-established route is to study dynamical heterogeneities, i.e., wide variations in the local mobility of the medium between different samples [39–43]. A first encouraging information comes by analyzing the difference in the msd of 100 particles randomly picked, uniformly in space, in the whole system. Figure 5 indicates that the dense case, with respect to the diluted one, exhibits a much wider volatility of msd. Such heterogeneity is large at intermediate times $t \sim t_{\text{cage}}$ and rapidly decreases at late times, i.e., when superdiffusion sets in. This confirms that superdiffusion is related to a strong coordination in the trajectories of particles.

In conclusion, we demonstrate that probe’s anomalous diffusion originates in a collective mode of the host granular medium, even if it is constituted of many nonpolar particles. The slow component of the grains’ movement along a direction which is free of obstacles, i.e., rotation around the central axis, is more and more coordinated and persistent as density increases and temperature decreases. The observed strong and enduring correlations are not particularly sensitive to changes in the dissipation and in the size of the system and, noticeably, to the degree of configurational (e.g., crystalline) order, see the Supplemental Material [21]. The robustness of our results suggests that they could apply to other systems, for instance granular materials under different conditions of

fluidizations, as well as disordered glassy systems and fluids of active particles. The dynamical memory displayed by our system could be a more easy way to observe proxy for very slow configurational relaxation in hard sphere glasses [44]. Moreover, persistent alignment of velocities of inertial active particles is observed in animal collective behavior, such as in flocks [45]. While its theoretical connection with granular materials is established [46,47], our Letter supports the experimental grounds for the development of a common physical understanding of such diverse systems.

-
- [1] H. M. Jaeger, S. R. Nagel, and R. P. Behringer, *Rev. Mod. Phys.* **68**, 1259 (1996).
- [2] B. Andreotti, Y. Forterre, and O. Pouliquen, *Granular Media* (Cambridge University Press, Cambridge, England, 2013).
- [3] N. Brilliantov, P. Krapivsky, A. Bodrova, F. Spahn, H. Hayakawa, V. Stadnichuk, and J. Schmidt, *Proc. Natl. Acad. Sci. U.S.A.* **112**, 9536 (2015).
- [4] *Granular Gas Dynamics*, edited by T. Pöschel and N. V. Brilliantov (Springer, Berlin, 2003), pp. 293–316.
- [5] A. R. Abate and D. J. Durian, *Phys. Rev. Lett.* **101**, 245701 (2008).
- [6] C. Ness, R. Mari, and M. E. Cates, *Sci. Adv.* **4**, eaar3296 (2018).
- [7] N. V. Brilliantov and T. Pöschel, *Kinetic Theory of Granular Gases* (Oxford University Press, Oxford, 2004).
- [8] A. Puglisi, *Transport and Fluctuations in Granular Fluids* (Springer-Verlag, Berlin, 2015).
- [9] Y. Forterre and O. Pouliquen, *Annu. Rev. Fluid Mech.* **40**, 1 (2008).
- [10] A. Puglisi, A. Gnoli, G. Gradenigo, A. Sarracino, and D. Villamaina, *J. Chem. Phys.* **136**, 014704 (2012).
- [11] B. Kou, Y. Cao, J. Li, C. Xia, Z. Li, H. Dong, A. Zhang, J. Zhang, W. Kob, and Y. Wang, *Nature (London)* **551**, 360 (2017).
- [12] A. Puglisi, A. Baldassarri, and A. Vulpiani, *J. Stat. Mech.* (2007) P08016.
- [13] A. Sarracino, D. Villamaina, G. Gradenigo, and A. Puglisi, *Europhys. Lett.* **92**, 34001 (2010).
- [14] A. Gnoli, A. Puglisi, A. Sarracino, and A. Vulpiani, *PLoS One* **9**, e93720 (2014).
- [15] K. Feitosa and N. Menon, *Phys. Rev. Lett.* **88**, 198301 (2002).
- [16] C. Scalliet, A. Gnoli, A. Puglisi, and A. Vulpiani, *Phys. Rev. Lett.* **114**, 198001 (2015).
- [17] A. Lasanta and A. Puglisi, *J. Chem. Phys.* **143**, 064511 (2015).
- [18] G. Briand, M. Schindler, and O. Dauchot, *Phys. Rev. Lett.* **120**, 208001 (2018).
- [19] B. Kou, Y. Cao, J. Li, C. Xia, Z. Li, H. Dong, A. Zhang, J. Zhang, W. Kob, and Y. Wang, *Phys. Rev. Lett.* **121**, 018002 (2018).
- [20] S. Plimpton, *J. Comp. Phys.* **117**, 1 (1995).
- [21] See Supplemental Material at <http://link.aps.org/supplemental/10.1103/PhysRevLett.123.038002> for details on analytical and numerical results, which includes Refs. [20,22–35].
- [22] F. Lechenault, R. Candelier, O. Dauchot, J.-P. Bouchaud, and G. Biroli, *Soft Matter* **6**, 3059 (2010).
- [23] H. P. Zhang and H. A. Makse, *Phys. Rev. E* **72**, 011301 (2005).
- [24] L. E. Silbert, D. Ertz, G. S. Grest, T. C. Halsey, D. Levine, and S. J. Plimpton, *Phys. Rev. E* **64**, 051302 (2001).
- [25] N. V. Brilliantov, F. Spahn, J. M. Hertzsch, and T. Pöschel, *Phys. Rev. E* **53**, 5382 (1996).
- [26] V. L. Popov, *Contact Mechanics and Friction* (Springer-Verlag, Berlin, 2010).
- [27] A. Di Renzo and F. P. Di Maio, *Chem. Eng. Sci.* **59**, 525 (2004).
- [28] T. S. T. Pöschel, *Computational Granular Dynamics* (Springer, Berlin, 2005).
- [29] M. Rackl and K. J. Hanley, *Powder Tech.* **307**, 73 (2017).
- [30] W. Lechner and C. Dellago, *J. Chem. Phys.* **129**, 114707 (2008).
- [31] J. Russo and H. Tanaka, *Sci. Rep.* **2**, 505 (2012).
- [32] E. Zaccarelli, C. Valeriani, E. Sanz, W. C. K. Poon, M. E. Cates, and P. N. Pusey, *Phys. Rev. Lett.* **103**, 135704 (2009).
- [33] P. Pusey, E. Zaccarelli, C. Valeriani, E. Sanz, W. C. Poon, and M. E. Cates, *Phil. Trans. R. Soc. A* **367**, 4993 (2009).
- [34] W. Brenig, Hydrodynamic long-time tails, in *Statistical Theory of Heat* (Springer, New York, 1989), p. 149.
- [35] A. Fiege, T. Aspelmeyer, and A. Zippelius, *Phys. Rev. Lett.* **102**, 098001 (2009).
- [36] A. Sarracino, D. Villamaina, G. Costantini, and A. Puglisi, *J. Stat. Mech.* (2010) P04013.
- [37] A. Gnoli, A. Puglisi, and H. Touchette, *Europhys. Lett.* **102**, 14002 (2013).
- [38] Our analysis revealed that the behavior of the granular medium is largely independent from the presence or absence of the blade, however a blade-free simulation seemed us *cleaner* with respect to assessing the minimal ingredients of the observed dynamics.
- [39] M. D. Ediger, *Annu. Rev. Phys. Chem.* **51**, 99 (2000).
- [40] L. Berthier, G. Biroli, J.-P. Bouchaud, L. Cipelletti, and W. van Saarloos, *Dynamical Heterogeneities in Glasses, Colloids, and Granular Media* (Oxford University Press, Oxford, 2011), Vol. 150.
- [41] O. Dauchot, G. Marty, and G. Biroli, *Phys. Rev. Lett.* **95**, 265701 (2005).
- [42] A. S. Keys, A. R. Abate, S. C. Glotzer, and D. J. Durian, *Nat. Phys.* **3**, 260 (2007).
- [43] R. Candelier, O. Dauchot, and G. Biroli, *Phys. Rev. Lett.* **102**, 088001 (2009).
- [44] D. V. T. G. G. Gradenigo, A. Sarracino, and A. Puglisi, *J. Stat. Mech.* (2010) L12002.
- [45] A. Cavagna, I. Giardina, and T. S. Grigera, *Phys. Rep.* **728**, 1 (2018).
- [46] A. Manacorda and A. Puglisi, *Phys. Rev. Lett.* **119**, 208003 (2017).
- [47] A. Manacorda, *Lattice Models for Fluctuating Hydrodynamics in Granular and Active Matter* (Springer, New York, 2018).